

FABRICATION AND SIMULATION OF A PZT ENERGY HARVESTER MEMS

G. A. Ardila Rodríguez¹, H. Durou¹, L. Ourak¹, D. Colin¹, C. Rossi¹, C. Baud¹, J. Y. Fourniols^{1,2}

¹LAAS-CNRS; Université de Toulouse; 7 avenue du colonel Roche, 31077 Toulouse Cedex 04, France

²Université de Toulouse; INSA

Abstract: In this paper we present the design, fabrication and characterization of a harvesting device designed to power wireless sensors network for aircraft Structure Health Monitoring. It is designed to harvest mechanical vibrations produced by the aircraft engine (0.01 to 0.1g at 50Hz) to produce enough electrical power (a few μW , 9V) for sensor supply. A 4 serial-connected cantilever structure with 200 μm thick PZT films can deliver 2.95 μW and 9.42V over an optimal resistive load (25M Ω) under 0.1g and 50Hz.

Key words: Energy harvesting, MEMS, FEM modeling, PZT

1. INTRODUCTION

Remote wireless networks are a very attractive and flexible technology for applications requiring embedded sensors in inaccessible locations.

One of the possible applications of wireless networks is the Aircraft Structure Health Monitoring (SHM) [1]. This application imposes inherent constraints (vibration frequency and level) and some limiting geometric constraints (thickness) to avoid aircraft aerodynamics alterations.

The use of batteries having short lifespan is a high limitation for SHM wireless sensing networks. One emerging option is to harvest the ambient energy (vibration [2], light [3, 4] or heat [5]) to make the system completely autonomous over a theoretical infinite lifespan. A typical harvesting system is composed of 3 parts: 1) the harvesting part, 2) the AC-DC electrical conversion allowing to efficiently recover the energy and 3) the storage devices (Fig. 1).

This article details the design, modeling and fabrication of the harvesting part which is based on piezoelectric vibration to electrical conversion.

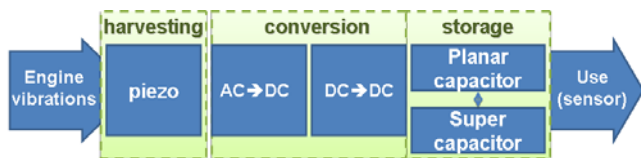


Fig. 1: Harvesting system main parts.

2. DESIGN AND MODELING

Our structure consists in 4 serial-connected PZT cantilevers with a shared proof mass of 8g (Fig. 2). This design permits to amplify the voltage level supplied by the device compared to a one cantilever design. The total surface of the system is limited to

5cm² and its thickness to 2.5mm to avoid aircraft aerodynamics alteration.

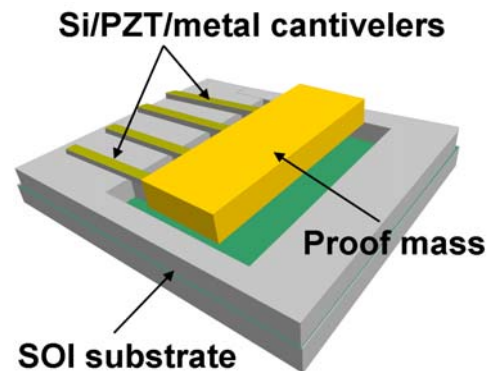


Fig. 2: Structure of the PZT energy harvester.

2.1 FEM modeling

Mechanical simulations using FEM modeling under COMSOL Multiphysics permit to optimize the dimensions of the cantilevers to fit the application requirements which are: vibration main frequency of 50Hz and maximal acceleration of 0.1g. The system must generate enough voltage to pass the threshold voltage of a typical diode in an AC-DC converter ($\approx 0.6\text{V}$). The optimal structure has a cantilever width of 350 μm , length of 15mm and PZT/Si thicknesses 200 μm /100 μm . FEM mechanical simulations show that the maximal mechanical stresses at the cantilever fixed end is lower than 50MPa at 0.1g and 50Hz.

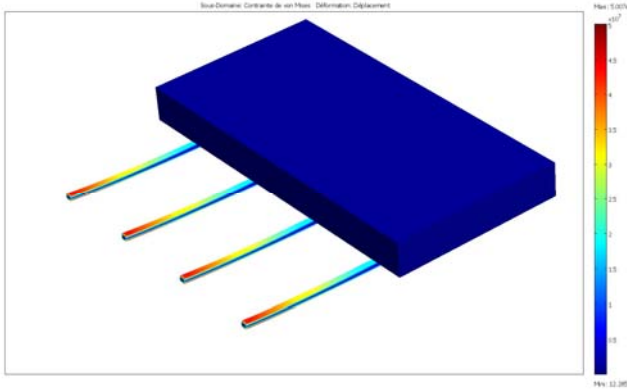


Fig. 3: COMSOL implemented model of a 4 cantilevers system with 8g proof mass. The model shows the maximal produced stress of 50MPa at the fixed end.

2.2 System modeling

To fully optimize the harvesting system, a linked COMSOL and VHDL-AMS (System Vision) simulation has been implemented and permits to calculate the electrical power and voltage over an optimal resistive load as a function of the PZT layer thickness.

Based on this study (see table 1) we have chosen a 200 μ m thick PZT film and a 4 cantilevers structure to fabricate a first prototype.

Table 1: Power performances as a function of PZT thickness for the 4 cantilevers structure.

| PZT thickness (μ m) | Max. Power (μ W) |
|--------------------------|-----------------------|
| 100 | 3.06@3.91V |
| 200 | 2.95@9.42V |
| 300 | 2.04@14.3V |
| 400 | 1.04@14.5V |

An image of the implemented VHDL-AMS model is presented in Figure 4.

A VHDL-AMS one cantilever model was implemented following the constitutive equations:

$$\begin{aligned} D &= a_{11}F + a_{12}V \\ I &= a_{21}\frac{\partial F}{\partial t} + a_{22}\frac{\partial V}{\partial t} \end{aligned} \quad (1)$$

With D, F, V and I being (respectively) the deformation of the cantilever, the force applied to it, the Voltage across its poles and the current flowing through. These equations require additional parameters [6]:

$$\begin{aligned} a_{11} &= \frac{4S_{11_PZT}S_{11_Si}(S_{11_PZT}t_{Si} + S_{11_Si}t_{PZT})L^3}{Kw} \\ a_{12} &= \frac{-3d_{31}S_{11_PZT}S_{11_Si}t_{Si}(t_{Si} + t_{PZT})L^2}{K} \\ a_{21} &= a_{12} \\ a_{22} &= \frac{Lw(\epsilon - d_{31}^2t_{Si}(S_{11_PZT}t_{Si}^3 + S_{11_Si}t_{PZT}^3))}{t_{PZT}K} \end{aligned} \quad (2)$$

$$S_{11_PZT} = \frac{1}{E_{PZT}}$$

$$S_{11_Si} = \frac{1}{E_{Si}}$$

$$\epsilon = \epsilon_0\epsilon_r \quad (3)$$

$$\begin{aligned} K &= S_{11_PZT}S_{11_Si}t_{Si}t_{PZT}(4t_{PZT}^2 + 4t_{Si}^2 + 6t_{Si}t_{PZT}).. \\ &+ S_{11_Si}^2t_{PZT}^4 + S_{11_PZT}^2t_{Si}^4 \end{aligned}$$

L, w and t are (respectively) the length, width and thickness of the films, E the Young modulus and ϵ the permittivity.

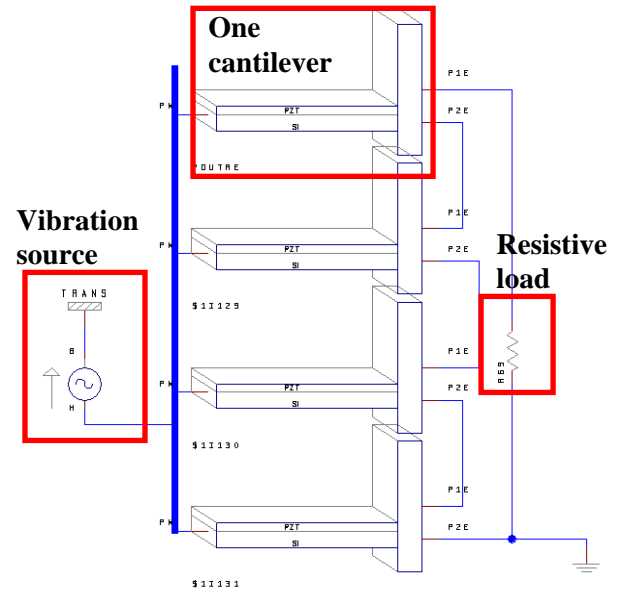


Fig. 4: Implemented VHDL-AMS model of 4 serial-connected cantilevers with an optimised resistive load.

The modeling results (Fig. 5) show that using a 200 μ m thick PZT layer, the expected maximal power is of 2.95 μ W under an acceleration of 0.1g at 50Hz. That corresponds to a voltage of 9.42V across a resistive optimal charge of 25M Ω .

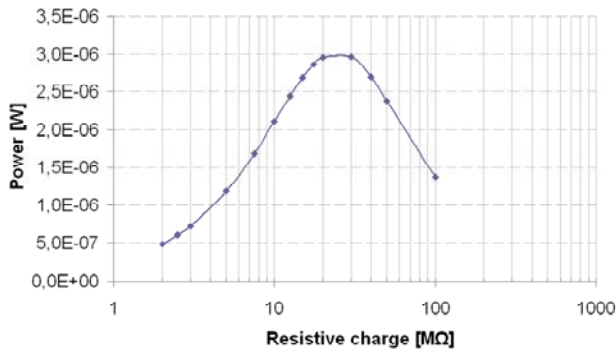


Fig. 5: Generated electrical power in function of the resistive charge.

3. FABRICATION

The fabrication process starts from a 4” SOI (Silicon On Insulator) substrate and uses simple MEMS process steps. It can be summarized as follows (Fig. 6): 1) the first step is the deposition of thin films: a SiN_x film (0.15μm) for electrically insulate the substrate (SOI) and a Ti/Au film (0.1μm/0.8μm) to create the metallic contacts (Fig. 6a). 2) The second step consists in successive plasma etching: RIE (Reactive Ion Etching) of the deposited SiN_x on both wafer sides and the SOI oxide (SiO₂), and DRIE (Deep Reactive Ion Etching) of the Si (100μm) that will further create the cantilevers (Fig. 6b). 3) The next step is the manual placement and bonding of a 200μm thick PZT film (610-HD supplied by TRS Technologies) using a Tresky 3000 machine. The PZT film is previously metalized with Cr/Au (500A/5000A) (Fig. 6c). This PZT was chosen for its relatively high d₃₃ and d₃₁ coefficients (690pC/N and -340pC/N respectively) [7]. 4) Then the PZT is laser etched around the cantilevers using a femtosecond laser (Fig. 6d) chosen for its low temperature characteristics. 5) The fifth step is the manual placement and bonding of the proof mass (W₁ and W₂) on the cantilevers (Fig. 6e). 6) The cantilevers are liberated from the substrate with a chemical anisotropic etching bath (KOH) (Fig. 6f). 7) The last step is the electrical serial connections between the cantilevers (Fig. 6g).

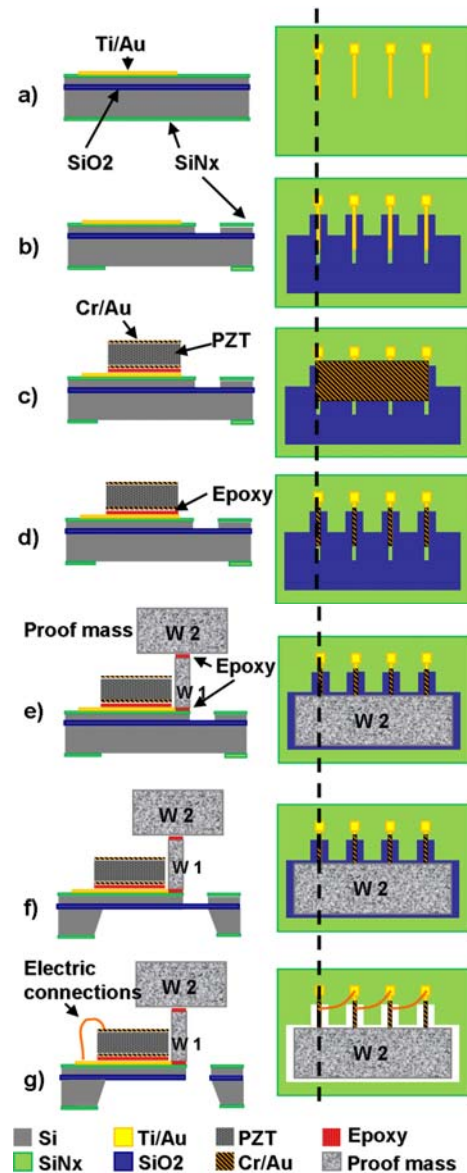


Fig. 6: Main fabrication steps of the vibration harvester. Cut view and top side view. a) Thin film deposition. b) RIE/DRIE etching. c) PZT film placement. d) PZT laser etching. e) Proof mass placement. f) KOH backside etching. g) Electrical connections.

Photos of the first prototype fabrication steps are presented in Fig. 7 and Fig. 8.

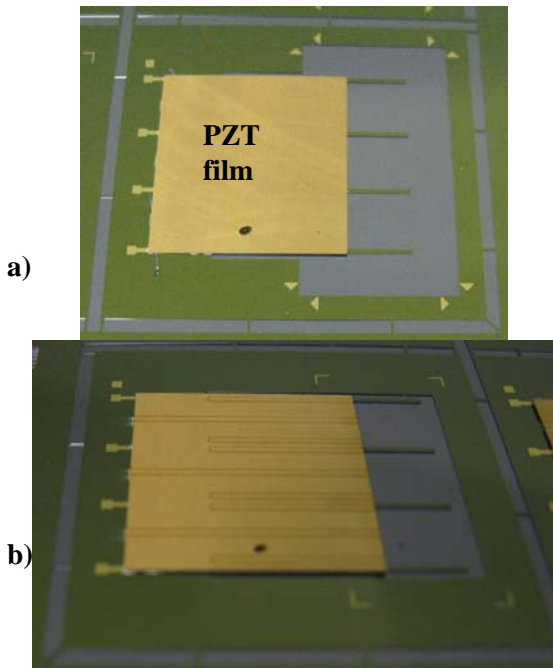


Fig. 7: Photo of realizations. a) PZT film placement over the MEMS structure. b) Laser etching of the PZT film.

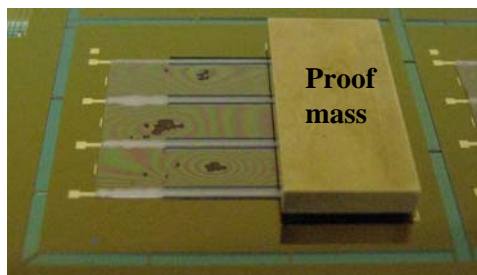


Fig. 8: Realization images. a) PZT film placement over the MEMS structure. b) Proof mass placement.

4. DISCUSSION

The fabrication scheme of the prototype presents several drawbacks. Manual placement of the different parts (PZT film, proof masses) should be improved by using a flip-chip machine for example.

The laser etching is one of the principal difficulties encountered in the prototype fabrication. The laser etching line a single line presents a very narrow width ($\approx 20\mu\text{m}$) that makes the delimited piece difficult to be removed. An optimized etching process is currently under study: increase the laser energy is required to fully reach the bottom end of the PZT film. Multiple successive laser lines must also be patterned to remove easily the pieces. These last results will be presented at the conference meeting together with the characterization results.

5. CONCLUSIONS AND PERSPECTIVES

Design, optimization through modeling (COMSOL and VHDL-AMS) and fabrication of a PZT energy harvester is presented for aircraft SHM applications, though it could be used in multiple wireless networks applications where mechanical vibrations are available. The chosen 4 serial-connected cantilever structure increases the power and voltage compared to a single cantilever structure.

Technical problems concerning the laser etching have been encountered and are now overcome; for this reason the first characterization results will be presented in the conference meeting.

Future work concerns the fully system simulation and fabrication including multi-source harvesting (mechanical vibrations, thermal variations, light, etc) the conversion and energy storage harvesting parts (planar and/or super capacitors).

ACKNOWLEDGEMENTS

The authors would like to thank the Aerospace Foundation (FRAE) for supporting this research. We also like to thank the TEAM service and X. Dollat from the LAAS-CNRS laboratory for their services. Finally we thank ALPhANOV for their services in laser etching.

REFERENCES

- [1] Giurgiutiu V, Zagari A and Bao J 2002 Piezoelectric Wafer Embedded Active Sensors for Aging Aircraft Structural Health Monitoring *Structural Health Monitoring*. **1** 41-61
- [2] Beeby S P, Tudor M J, White N M 2006 Energy harvesting vibration sources for microsystems applications *Measurement Science and Technology*. **17** R175-R195
- [3] Voigt T, Ritter H, Schiller J Utilizing solar power in wireless sensor networks *Proceedings 28th IEEE Int. Conf. on Local Computer Networks (2003)* 416-422
- [4] Raghunathan V *et al* Design considerations for solar energy harvesting wireless embedded systems *Proceedings of the 4th Int. Symposium on Information Processing in Sensor Networks (2005)* 457-462
- [5] Sodano H A *et al* 2007 Recharging Batteries using Energy Harvested from Thermal Gradients *Journal of Intelligent Material Systems and Structures* **18** 3-10
- [6] Smits J G, Choi W-S 1991 The Constituent Equations of Piezoelectric Heterogeneous Bimorphs *IEEE Transactions on Ultrasonics, Ferroelectrics and Frequency Control* **38** 256-270
- [7] TRS Technologies, Inc. - Piezoelectric Materials Datasheet; <http://www.trstechnologies.com/Materials/Piezoceramics/properties.php>, Webpage accessed on September 30, 2008.